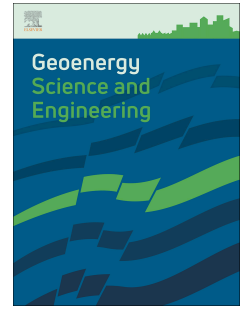


Journal Pre-proof



Fracture toughness tests of shale outcrops: Effects of confining pressure

Fabián J. Antinao Fuentealba, Gonzalo Blanco, Leandro N. Bianchi, José L. Otegui, Gustavo L. Bianchi

PII: S2949-8910(23)01041-2

DOI: <https://doi.org/10.1016/j.geoen.2023.212454>

Reference: GEOEN 212454

To appear in: *Geoenergy Science and Engineering*

Received Date: 1 May 2023

Revised Date: 10 October 2023

Accepted Date: 30 October 2023

Please cite this article as: Antinao Fuentealba, Fabián.J., Blanco, G., Bianchi, L.N., Otegui, José.L., Bianchi, G.L., Fracture toughness tests of shale outcrops: Effects of confining pressure, *Geoenergy Science and Engineering* (2023), doi: <https://doi.org/10.1016/j.geoen.2023.212454>.

This is a PDF file of an article that has undergone enhancements after acceptance, such as the addition of a cover page and metadata, and formatting for readability, but it is not yet the definitive version of record. This version will undergo additional copyediting, typesetting and review before it is published in its final form, but we are providing this version to give early visibility of the article. Please note that, during the production process, errors may be discovered which could affect the content, and all legal disclaimers that apply to the journal pertain.

© 2023 Published by Elsevier B.V.

Fracture toughness tests of shale outcrops: effects of confining pressure

Fabián J. Antinao Fuentealba^{*ad}, Gonzalo Blanco^{ab}, Leandro N. Bianchi^c, José L. Otegui^{ab},
Gustavo L. Bianchi^{ab}

^a Innovation for Energy and Environment, Malvinas Institute. Faculty of Engineering, National University of La Plata, Argentina.

^b National Scientific and Technical Research Council (CONICET), Argentina.

^c Solaer Ingeniería S.A, La Plata, Argentina.

Tecticons South S.A ^d

*corresponding author: fabian.antinao@ing.unlp.edu.ar

Abstract

Brittle rock fracture is a core concept in oil and gas and other rock mechanics projects. However, the understanding of fracture behavior under mechanical well-bottom conditions remains insufficient. This article aims to analyze experimental results for the critical stress intensity factor (K_{IC}) of outcrops from Vaca Muerta carbonate-rich shale rocks, tested under a range of crack depths and confining pressures (0 to 70 MPa). Fracture toughness (K_{IC}) is determined in multi-notched 1.5" plugs using a novel experimental set up, in which the crack-driving-force K_I and the confinement pressure are both applied by hydraulic systems. Finite fracture-mechanics-based models are used to calculate K_I . Our experimental results show that tests carried out at well-bottom pressures lead to apparent rock toughness doubling those for tests at atmospheric pressure.

Stress analysis demonstrates that the size of the tensile stressed zone ahead of the crack tip tends to decrease as confining pressure increases. Additionally, compressive deviatoric stresses are developed ahead of the tensile zone, with their magnitude being dependent on the level of confinement. Moreover, triaxial stress states induced by confinement could lead to microcracking ahead of the crack tip. The mechanisms of crack closure and deviatoric stress-induced microcrack initiation are combined to assess a plausible mechanism for rock toughness enhancement under confined conditions. It is concluded that increasing triaxial pressure confinement allows to accurately model the mechanical response of shale rocks under reservoir conditions.

Key words: shale rocks; fracture test; toughening mechanism; Vaca Muerta, microcracking

Nomenclature, list of acronyms and units

a	Crack length (mm)
D	Diameter (mm)
a/D	Crack ratio (dimensionless)
FE	Finite element
HF	Hydraulic fracture
SRV	Stimulated Reservoir Volume
LEFM	Linear Elastic Fracture Mechanics
SIF	Stress Intensity Factor
K_{IC}	Mode I Fracture toughness ($\text{MPa}\cdot\text{m}^{1/2}$)
K_I	Applied stress intensity factor ($\text{MPa}\cdot\text{m}^{1/2}$)
FPZ	Fracture process zone
RBSN	Round bar Straight notch specimen
P_i	Inner pressure (MPa)
P_c	Confining or outer pressure (MPa)
ΔP_r	Pressure differential at the break event (MPa)
F_p	Dimensionless-SIF or geometry factor
σ	Nominal stress away from the crack tip (MPa)
UC, MC and HC	Unconfined, middle and high confinement conditions
$S_{xx}, S_{yy},$ S_{zz}	Principal stresses (MPa)
CZ	Cohesive zone
r_y	Distance from the crack tip along 'Y' coordinate (mm)

1. INTRODUCTION

The fluid-driven hydraulic fracture (HF) is a technique to improve hydrocarbon production from low permeability reservoirs. Its development and optimization date back to the 1940s, and it has been increasingly implemented in unconventional oil and gas reservoirs over the last three decades (Smith and Montgomery, 2015). The primary aim of HF is to increase the Stimulated Reservoir Volume (SRV) by creating tensile fractures through high-pressure fluid injection in a coupled hydro-mechanical process (Heng et al., 2021; Zhong et al., 2018).

At field scale, there are many geotechnical and geomechanical processes where the critical fracture parameters are governed by tensile strength. Considering that this mechanical property is lower than compression strength, areas under tensile stresses are particularly prone to initiating tensile failure (Xu et al., 2018). Particularly, the HF process is mainly driven by tensile strength; thus, it is an important aspect of the resistance to failure of a rock (Perras and Diederichs, 2014).

A well-known approach for analyzing fracture processes is Linear Elastic Fracture Mechanics (LEFM). It is based on the concept of the crack-tip Stress Intensity Factor (SIF or K_I), usually measured in Mode I (tensile crack opening). In laboratory experiments, LEFM allows for the determination of the fracture toughness K_{IC} , which is the maximum value of applied K_I and a material property of the tested rock. Toughness is a basic concept in fracture mechanics that provides a physical framework for understanding many processes associated with rock fractures. It measures rock resistance to brittle propagation and failure, and it is related to the energy absorbed by the rock during those stages (Gudmundsson, 2011). In the field of rock

mechanics, particular attention has been given to studying Mode I fractures, where the stress that triggers propagation is perpendicular to the initial crack surface. This focus is primarily due to the tensile strength of rock materials, which is typically lower than their compressive strength (Jaeger, 2007).

Both conventional and unconventional underground energy sources have required the use of the LEFM approach to model and predict, or at least, estimate the behavior of fracture processes (Jin et al., 2014; Razavi et al., 2017). For instance, in-situ stress measurement (Amadei and Stephansson, 1997; Mohamadi et al., 2021), breakdown pressure prediction (Chen et al., 2022; Lu et al., 2022; Sapore et al., 2023; Q. Zhang et al., 2020), breakout failure estimation (Dresen et al., 2010; Lin et al., 2020), fracture gradient analysis (Gao et al., 2020; Mirabbasi et al., 2020), and hydraulic fracture propagation analysis (Lecampion et al., 2018; Wang, 2015) have been studied through LEFM approach.

While experimental and numerical techniques have been proposed to model these stages, progress has been hindered by several challenges, such as the lack of knowledge about real rock mechanical properties, stress states and scale dependency (Fan et al., 2019), and uncertainties related to non-linear rock behavior (Dutler et al., 2018). Therefore, it is of paramount importance to comprehensively understand the mechanisms that govern toughness under actual well-bottom conditions, especially considering the influence of confining pressure.

1.1 Experimental fracture toughness determination

Core specimens are frequently used to study fracture toughness in quasi-brittle materials under atmospheric pressure conditions, and international standards recommend the use of only four specimens for fracture testing (Dai et al., 2015). Although confined tests are not standardized, different specimen geometries have been employed for Mode I testing, as summarized in Table 1. The applied K_I is regularly transferred through mechanical contact, while the confining stress is transmitted by an external fluid. In contrast, the notched thick-walled cylinder is one of the few techniques that applies a fluid pressure as driving-force. Confined test methods comprise typically the use of jacketed surface notches to elude the modification of stress distribution or chemo-physical damage near the crack tip.

Regarding the rock material, most of the experimental measurements documented in Table 1 and illustrated in Fig. 1 utilized outcrop specimens. This preference is common due to its cost-effectiveness and the availability of samples for analysis, especially when compared to the more complex process of acquiring core data. However, it is acknowledged that the burial history and diagenesis of outcrop and subsurface shale formations diverge, resulting in distinct impacts on petrophysical properties in samples. Further details regarding the differences between these two sources of rock samples can be explored in Sharifigaliuk et al. (2021).

As we delve deeper into the rock damage and fracture process, it is accepted that various stages of those processes involve microfracture development and interactions. Both outcrop and subsurface samples undergo distinct processes, including tectonic activities, diagenesis, mineralogical transformations, hydrocarbon generation, and maturation, all of which collectively contribute to the creation of microfractures. Moreover, shale outcrops in the near-surface are susceptible to weathering, a phenomenon influenced by factors such as initial mineralogy, organic matter content and the interplay between different minerals. These factors significantly impact microfracture density, porosity, and pore size distribution.

The evaluation of fracture toughness in specimens may have biases from different experimental sources. These include the impact of friction at loading points on the samples (Liu et al., 2022) as well as the influence of confining pressure. Diverse studies have explored the influence of confinement on fracture toughness measurements. As it is shown in Fig. 1,

results obtained in the laboratory are consistent: as confining pressure increases, K_{IC} tends to rise, although the underlying mechanisms are still subject to debate (see references in Table 1).

Considering that the fundamental mechanisms governing rock fracture are largely influenced by microfracturing, the intrinsic density of these microfractures within samples becomes a critical source of error. On a laboratory scale, discerning the true nature of microfractures identified in a rock sample is challenging. They might have originated either through exposure during the rock's burial or in the process of sampling. The open microfractures observed in outcrop shale samples might have been elastically closed under in situ conditions (Sharifigaliuk et al., 2021). Consequently, studies in fracture mechanics necessitate careful consideration of stress conditions, underscoring the importance of conducting experiments under representative confining conditions.

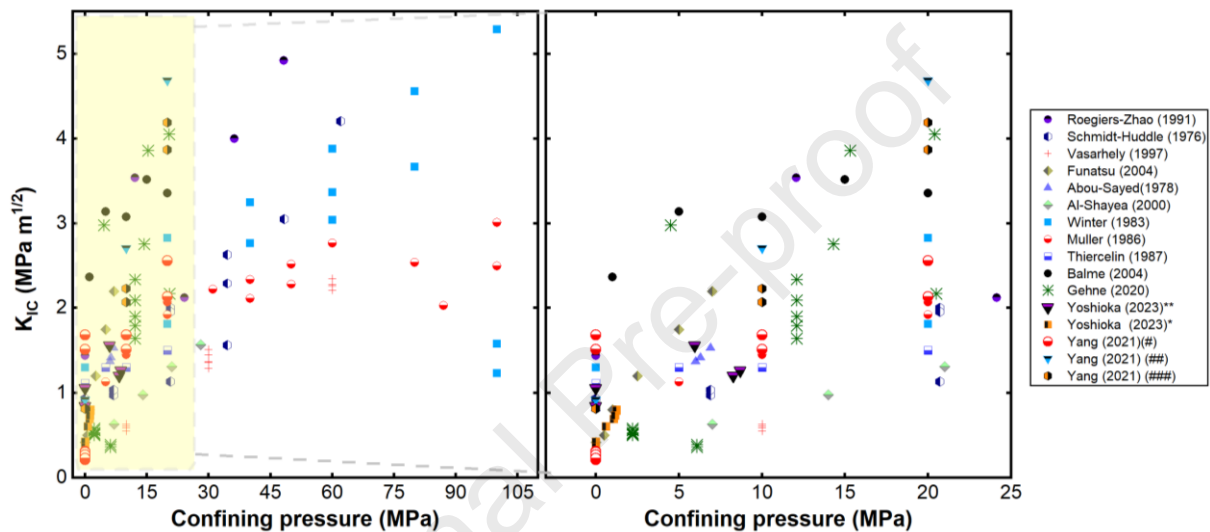


Figure 1: Experimental results of fracture toughness under confining pressure. References are shown in Table 1. See references and notes in supplementary data.

1.2 Effects of pressure on rock toughness

Given the significance of fracture toughness as a rock property, extensive efforts have been oriented to understanding rock behavior under well-bottom conditions. During the 1980s and 1990s, a series of publications by the Society of Petroleum Engineers (SPE) and other rock mechanics journals established the basis for the relationship between fracture toughness and confining pressure (Economides and Kenneth, 2000; Shlyapobersky, 1985; Shlyapobersky et al., 1988; Thiercelin, 1989). Afterward, various models and experimental tests yielded conflicting outcomes when comparing laboratory measurements of toughness to field extrapolations. Indirect in-situ measurements of rock toughness were performed, relying on recorded data of injected pressure and volume. Notably, the toughness estimated from these field tests demonstrated a magnitude range of 1-2 orders higher compared to laboratory measurements (Abou-Sayed et al., 1978; McClure et al., 2020; Zhu et al., 2022).

Numerous studies have attempted to elucidate the reasons behind the overestimation of breakdown pressure by fracture mechanics-based models, both at field and laboratory scales. In the first approach, some postulated mechanisms were fluid lag (Jeffrey, 2007), crack tip plasticity and dilatancy hardening induced by tensile or shear stresses (Yew and Liu, 1993), and frictional flow resistance (Van Dam and De Pater, 2001). Most toughness measurement techniques used in laboratory settings do not consider the influence of hydrodynamic

phenomena. Consequently, the intrinsic mechanisms behind these proposed mechanisms have not been fully explained.

Therefore, research efforts have been focused on investigating the underlying characteristics of rock fracture, particularly the effects of the fracture process zone (FPZ). Situated in proximity to the crack tip, the FPZ is a zone where extensive damage occurs because of the nucleation and coalescence of microcracks. The evolution of this zone significantly affects the overall fracture behavior and failure mechanisms exhibited by rocks (Garg et al., 2023) and introduces deviations from the fracture behavior predicted by LEFM (Nejati et al., 2020). At the same time, microcracks are a source of toughness enhancement (Dutler et al., 2018). Conceptually, rocks are tough because the cloud of cohesionless microcracks shields the principal notch from the externally applied stress field, so that the effective crack driving force dominating the stress field is smaller than that resulting from the applied loads (Hertzberg et al., 2012; K. Broberg, 1999). Both experimental and theoretical approaches have been employed to investigate microcrack shielding mechanisms in ceramic materials (Green, 2018).

The concept of microcracking induced by either FPZ development or deviatoric stress has been further explored by a few researchers. Swanson (1987) conducted fracture toughness tests in granite using a wedge-loaded double cantilever beam, measuring acoustic emission events. He found that the microcracking process increased fracture resistance and identified two potential toughening mechanisms: ligamentary bridging and frictional geometrical interlocking. Building on this article, Hashida et al. (1993) conducted fracture tests on granite under various confining pressures using a compact tension specimen and a cohesive zone model to predict breakdown pressure. They found that the size of the FPZ decreased when confinement increased. It is argued that under confinement, frictional interlocking was the main mechanism in the process zone, and confining pressure could enhance the frictional force induced by the compressive stress near the crack tip.

Furthermore, it has been observed that the application of deviatoric stresses can lead to the initiation and propagation of tensile microcracks, as evidenced in various stages of triaxial compressive tests, including crack closure, initiation, and damage (Paterson and Wong, 2005; Rahimzadeh Kivi et al., 2018). Fialko and Rubin (1997) conducted numerical stress analysis and performed simulations of thick-walled cylinders and compact tension specimens using cohesive models. Their findings demonstrated that the development of compressive stresses surrounding the FPZ could increase fracture energy. This enhancement was attributed to inelastic deformation occurring near the crack tip, resulting in an increased effective critical crack opening displacement and contributing to improved fracture resistance.

Another mechanism of toughness enhancement is crack closure. During fracture tests, confinement can generate negative applied stress intensity factor (K_I) values, leading to crack closure and inducing compressive stresses in the vicinity of the crack tip. Experimental (Funatsu et al., 2004; Gehne et al., 2020; H. Yang et al., 2021), analytical (Hammouda, 2022), and numerical models (Fialko and Rubin, 1997; Kataoka et al., 2017; H. Yang et al., 2021) were employed to calculate the applied K_I under confinement. Confinement plays a significant role in mitigating the initiation and propagation of cracks, thereby enhancing the strength of rocks. Within the framework of Linear Elastic Fracture Mechanics (LEFM), the application of compressive stresses to a crack results in a Mode I Stress Intensity Factor (SIF) that is either negative or zero, effectively inhibiting the formation of tensile microcracks in proximity to the crack tip.

Limited stress analysis has been conducted near the crack tip in confined experiments, leaving the validity of the linear elastic fracture mechanics (LEFM) hypothesis, the influence of deviatoric stresses near the crack tip, and the mechanism of toughness variation unexplored. This article presents experimental results for the critical stress intensity factor (K_{IC}) of Vaca Muerta shale rocks obtained from outcrops in the Neuquén basin, tested under realistic well-

bottom conditions. The experimental assessment of the effect of confinement pressure on fracture toughness is discussed in terms of K_{IC} results. Furthermore, the stresses near the crack tip are analyzed using finite element (FE) modeling with Abaqus. A potential mechanism based on the influence of deviatoric stresses and microcrack shielding is discussed to understand toughness-confinement dependency.

Journal Pre-proof

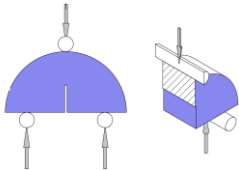
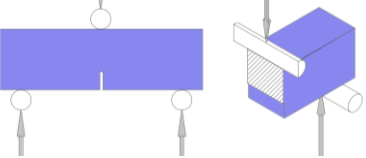
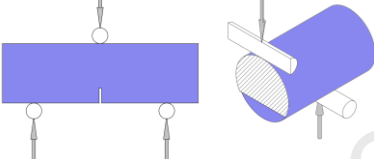
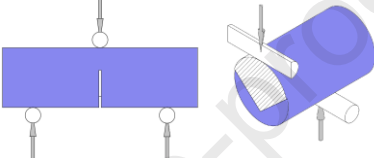
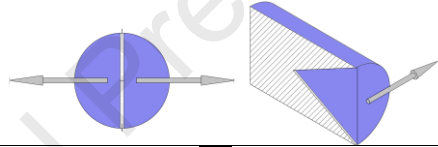
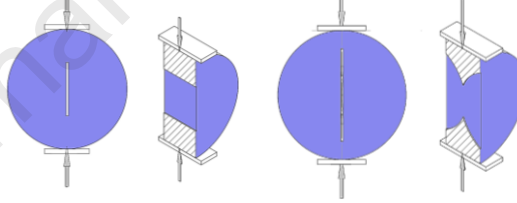
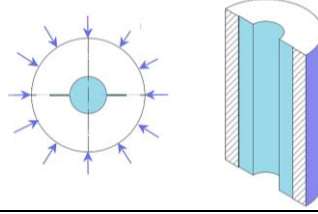
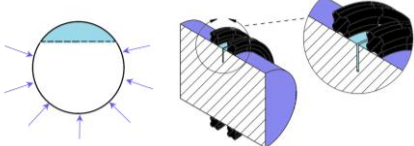
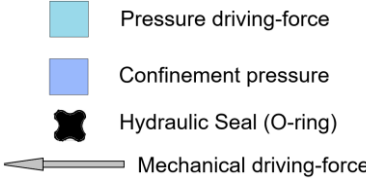




Load configuration	Geometry	Reference
Semi-circular bending (SCB)		(Funatsu et al., 2004; Kataoka et al., 2017; H. Yang et al., 2021; J. Yang et al., 2021)
Single edge notch bending (SENB)		(Müller, 1986; Vásárhelyi, 1997; Winter, 1983)
Single edge-notched round bar in bending (SENRBB / SECRBB)		(Funatsu et al., 2004; Müller, 1986; H. Yang et al., 2021)
Chevron bending (CB)		(H. Yang et al., 2021)
Short-rod (SR)		(Balme et al., 2004)
Cracked straight-through Brazilian disc method (CSTBD) - Cracked chevron notched Brazilian disc (CCNBD)		CSTBD: (Al-Shayea et al., 2000; Meng et al., 2018). CCNBD: (Ghanbari et al., 2019; Roegiers and Zhao, 1991)
Burst experiments / Thick-walled cylinder (TW)		(Abou-Sayed et al., 1978; Gehne et al., 2020; Shlyapobersky and Chudnovsky, 1994; Yoshioka et al., 2023)
Round bar Straight notch (RBSN)		(Antinao Fuentealba et al., 2022, 2020a)
Symbol reference	 <p>  Pressure driving-force  Confinement pressure  Hydraulic Seal (O-ring)  Mechanical driving-force </p>	

Table 1: Sample geometries frequently used in rock toughness tests under confining pressure.

2. EXPERIMENTAL METHODS

Specimen preparation, loading procedure and testing details have been previously described in other studies (Antinao Fuentealba et al., 2022, 2020b, 2020a). Carbonate-rich rock samples were taken from the Vaca Muerta outcrops, in the South-Central Neuquén basin in Argentina (Antinao Fuentealba et al., 2020a). Rocks were extracted according to their lamination directions. X-Ray Diffraction (XRD) results show that rocks have mainly high contents of calcite (89 %) and quartz (10 %), with clays percentage being lower than 1 % (smectite and feldspar).

RBSN specimens were used as test samples (Fig. 2), with diameter 'D' and crack length 'a'. Between 1 and 3 notches were cut in each plug (Fig. 2A), crack ratios were $0.1 < a/D < 0.25$, $D=38$ mm, and height between 20-35 mm. These samples were machined from outcrop block samples by a diamond core drill bit. Rock lamination or bedding planes were always kept perpendicular to crack planes in all samples. The plugs were dried in an oven at $45 \pm 2^\circ\text{C}$ for 24h. After ambient cooling, the samples were covered with a waterproof synthetic painting and varnish. The notches were machined with a 1 mm thick saw and finished with a 0.35 mm diamond wire. The procedure allows keeping the crack tip in contact with the fracture fluid:

- I) the synthetic painting is spread on plug surfaces and dried for 20 min.
- II) a pre-notch is machined with a saw up to a certain length.
- III) the varnish is applied on inner crack surfaces (Fig. 2B).
- IV) after 30min, the final notch is machined with a diamond wire up to 1 mm depth (Fig. 2C). This caused a blunt notch of ~ 0.4 mm. Painting and varnish ensure a proper sealing (minimizing the roughness in contact sample – O-ring) and minimize the interaction between the rock matrix and the fracture fluid.

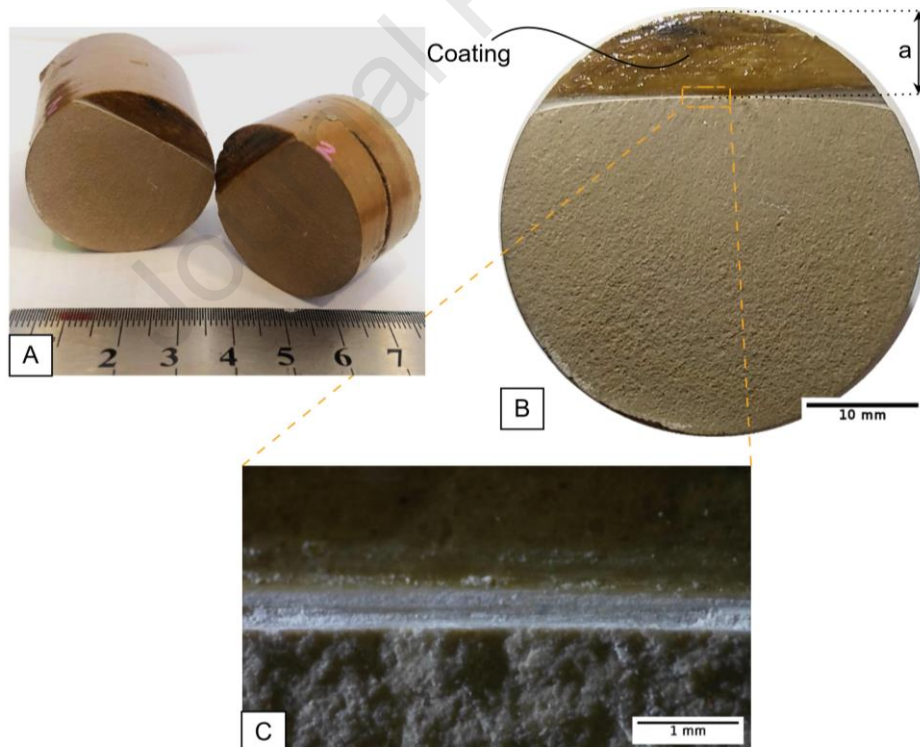


Figure 2: Multi-notched plug specimen. A) Coated round bar with straight-notch specimen. B) Coating and notch dimension on sample. C) Detail of notch tip, prefabricated with diamond wire.

During the rock fracture test, the machine simultaneously enables applying crack-opening and confining pressure (Fig. 3). The former is transferred inside a pre-existing crack, by pumping various fracture fluids at the inner pressure P_i (Fig. 3C-D). The confining pressure is pumped in a vessel enclosing the previous device (Fig. 3), where pressure and temperature are maintained with another (outer) fluid, matching well-bottom conditions, up to 90 °C and 80 MPa (maximum operating pressure). Both chambers are loaded with differential pressure $\Delta P = P_i - P_c$ until the break.

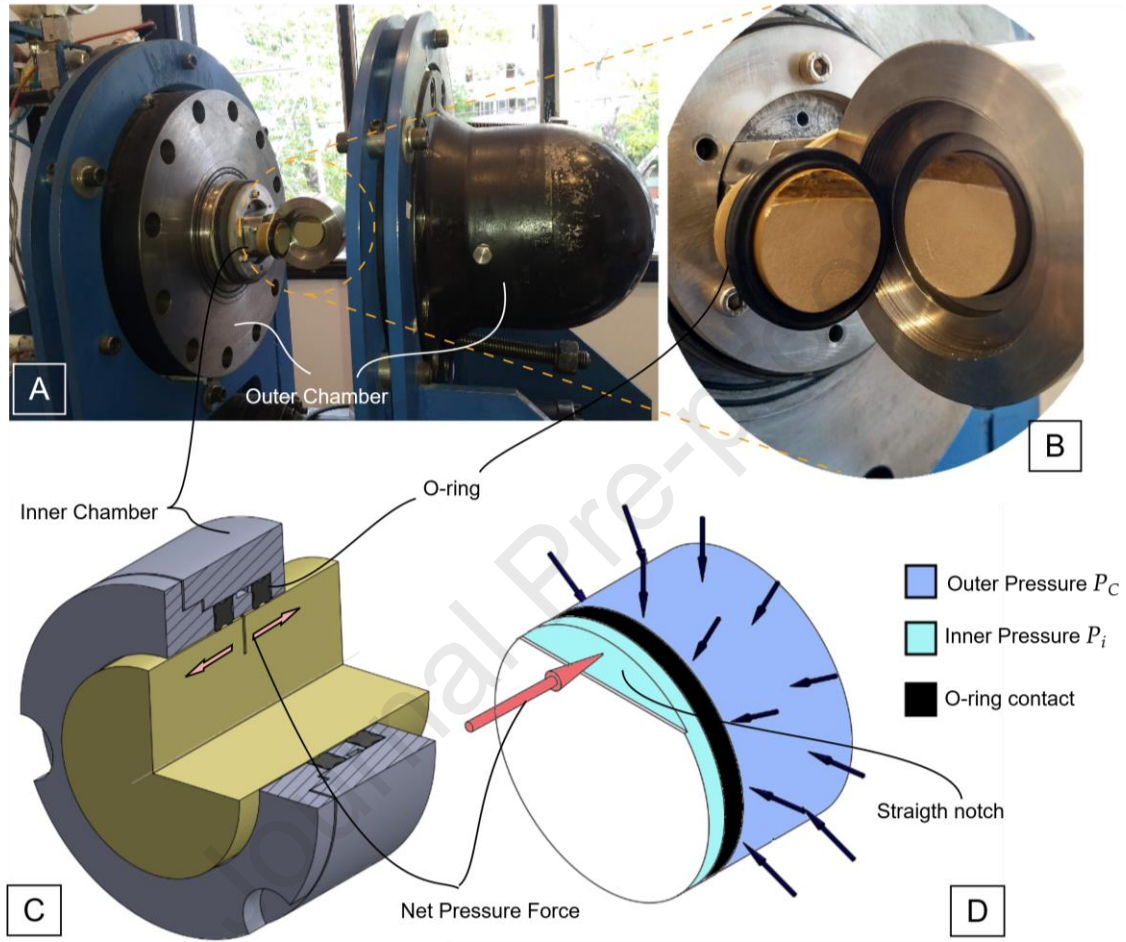


Figure 3: Experimental device for fracture toughness measurement. A) Inner and outer chamber. B-C) Detail of sample and O-ring arrangement on inner chamber. D) Schematic of boundary conditions on sample during fracture tests. Modified from (Antinao Fuentealba et al., 2022).

To determine the fracture toughness K_{IC} under confining pressure, eq. 1 is used:

$$K_{IC} = \Delta P_r \sqrt{\pi a} F\left(\frac{a}{D}\right) \quad (1)$$

Where ΔP_r is the pressure differential at the break event, a is the crack depth and D is the sample diameter. The pressure differential ΔP_r is detected as an instantaneous decreasing of pressure (see Fig. 5B in Antinao Fuentealba et al. (2022)). A dimensionless SIF is defined by $F\left(\frac{a}{D}\right)$, where $\frac{a}{D}$ is the crack ratio. The next expression of dimensionless-SIF was used for the calculations.

$$F_P\left(\frac{a}{D}\right) = 0.638 + 2.45 \left(\frac{a}{D}\right) - 0.637 \left(\frac{a}{D}\right)^2 \quad (2)$$

The term $F_p \left(\frac{a}{D} \right)$ is the dimensionless SIF obtained by polynomial fitting of numerical results ($R^2=0.99$) (Antinao Fuentealba et al., 2022). The values of F_p are 8 % lower than those reported by Toribio et al. (2009), for $0.1 < a/D < 0.5$.

The contribution of P_i and P_c in eq. 1 to total crack-driving force has been thoroughly analyzed (Antinao Fuentealba et al., 2022) by the J-integral method implemented in Abaqus (Dassault Systèmes, 2014; Pan et al., 2021; Wang et al., 2018). An isotropic rock was considered; elastic parameters are shown in Table 2 (Antinao Fuentealba et al., 2022). The dimensionless SIFs were calculated from 15 FE models for different conditions. According to Antinao Fuentealba et al. (2022) (Appendix A), the effects of O-ring forces on stress intensity factors (SIF) were insignificant.

The test program comprised 44 fracture tests, crack ratios were $0.1 < a/D < 0.25$, and the confining pressure were $P_c = 0, 20, 50, 70$ MPa. These pressure values were consistent with the in-situ stress magnitudes found in Vaca Muerta and other shale plays (Frydman et al., 2016; Michael and Gupta, 2020). It should be noted that this pressure spectrum was selected to encompass a wide range of potential fracture responses and tendencies observed in the experimental data.

3. RESULTS AND DISCUSSION

3.1. Experimental results for Vaca Muerta carbonatic shales

Fig. 4A displays the differential pressure ΔP_r in experimental fracture tests, as a function of confinement P_c and crack ratio a/D (scale of greys). Fig. 4B shows the results of experimental K_{IC} derived from eq. 1 and 2. Full data is supplied as supplementary data. K_{IC} in RBNS specimens is sensitive to crack ratio, especially for shallow cracks. By comparing tests with the same crack ratio and rising P_c from 0 to 70 MPa, Fig. 4A shows that ΔP_r increases by as much as 50 %. There is an apparent increase of K_{IC} with confinement, especially when $P_c < 50$ MPa, which is compatible with the current evidence (Funatsu et al., 2004; Ghanbari et al., 2019; Kataoka et al., 2017; H. Yang et al., 2021). For $P_c > 50$ MPa, the K_{IC} seems to be somehow invariant, being consistent with Funatsu et al.'s (2004) and H. Yang's (2021) findings. However, in those cases the confinement pressure transition was lower than 50 MPa, probably because different rock samples and specimen configurations were used.

The mechanism commonly mentioned to explain the sensitivity of fracture toughness with confining pressure is crack closure. Indeed, this phenomenon has been extensively researched in both conventional and true triaxial tests, by using mechanical and ultrasonic measurements (Hoek and Martin, 2014; Li et al., 2020; Taheri et al., 2020). Under LEFM approach, a crack loaded in compressive stresses has a negative or null Mode I SIF, avoiding the development of tensile microcracks near the crack tip.

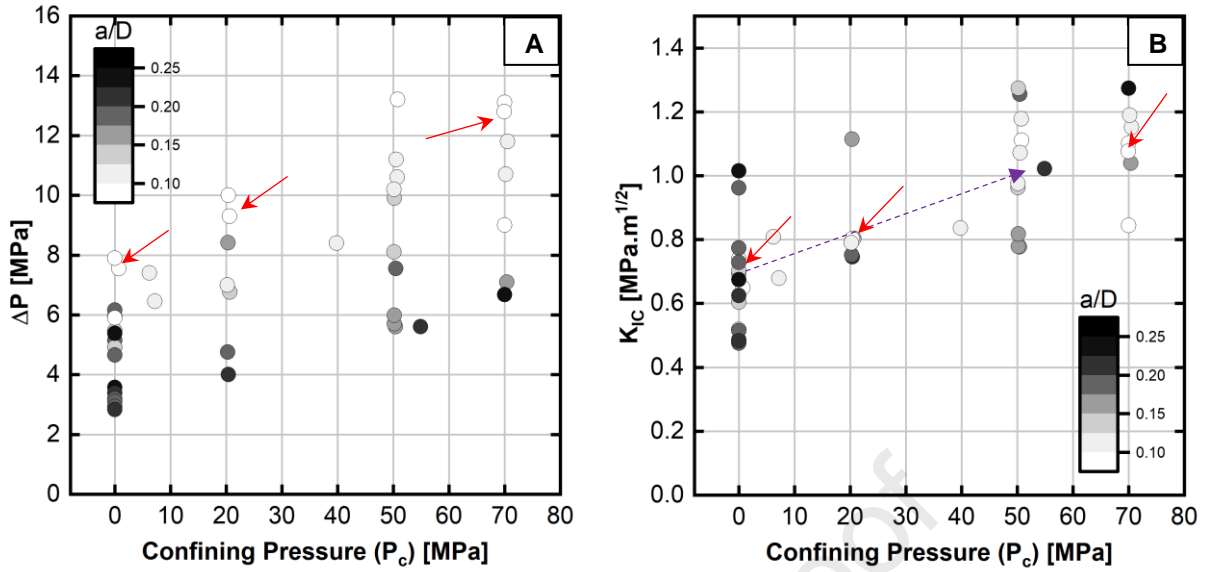


Figure 4: effect of confinement pressure ΔP and crack depth at fracture. A) differential pressure, B) fracture toughness. Red arrows indicate the fracture test condition for stress analysis in Section 3.2.

As pointed out by Yang et. al. (2021) and Kataoka et. al. (2017), FE modeling shows that compressive stress dominates a large part of the samples, causing high deviatoric stresses near the crack tip, even without bending stresses. Hou et al. (2017) conducted numerical analysis (XFEM or Extended finite element method, combined with the integral method) in CSTBD samples subjected to confinement. They found that Mode I SIF decreased as confining pressure increased, and that high confining pressure may even cause negative SIF, which should induce crack closure. Nevertheless, the stress analyses by FE fracture models were not conducted in those studies.

3.2. Effect of confinement pressure in SIF and fracture process zone

Mode I fracture in rocks is mainly controlled by tensile stresses in the crack tip. When the load rises, a highly stressed zone adjacent to the crack is developed, with inelastic deformation induced by microcracking damage. This place is the Fracture Process Zone (FPZ) and represents a mechanical property of the rock. LEFM methods rely in that both fracture toughness K_{IC} and tensile strength (TS) are independent of specimen and loading configuration (Dutler et al., 2018). However, according to eq. 1, fracture toughness in the RBSN specimen is controlled by P_c as well, which causes negative stress field near the crack tip. Thus, the compressive stresses could activate frictional mechanisms, and may influence the creation of microcracks outside the highly stressed region near the crack tip (Fialko and Rubin, 1997).

Several studies have determined the FPZ size by stress methods. Practical identification of FPZ involves knowledge of the field of stresses near the crack tip, obtained by FE models (Aliha et al., 2016; Pakdaman et al., 2019; Wei et al., 2021). In this scenario, Schmidt's formula is usually considered to define the size of FPZ (Schmidt, 1980), which adopts the rock's TS as the unique strength parameter to define FPZ size. Thus, the material volume where the tensile stress is greater than TS is considered as FPZ.

To analyze the behavior of FPZ under confined conditions, the principal stresses near the crack tip were considered in three tests (Fig. 4, red arrows), namely high confinement (HC), middle confinement (MC) and unconfined conditions (UC). The modeling technique was validated in Antinao Fuentealba et al. (2022). Table 1 shows the input parameter to calculate

the crack tip stresses. Following the coordinate system centered in point 'O' indicated in Fig. 5 and considering positive stresses in tension, the stress distributions are depicted in Fig. 6, with S_{xx} , S_{yy} , and S_{zz} .

In general, it can be seen that the stress fields are represented by triaxial stress states. For HC and MC tests (Fig. 6A), at distances greater than 0.07 mm, compressive stresses dominate the field stress. In unconfined tests (UC), the tensile stresses dominate at distances lower than 0.25 mm. This picture also shows the stress developing according to the definition of crack tip stresses dominated by SIF, described by eq. 9. From these results, it is evident that as confinement increases, the difference between the stress magnitudes dominated by K_I and those influenced by the confining pressure becomes more significant.

$$\sigma_{zz} = \frac{K_{IC}}{\sqrt{2\pi} r_y} \quad (3)$$

In order to assess the influence of confinement in FPZ size, let us examine Schmidt's criterion. Assuming rock TS is equal to 8 MPa (Antinao Fuentealba et al., 2020a; Massaro Sosa, 2019) and considering the stress distribution of S_{zz} in UC tests, the size of FPZ can be determined according to Schmidt's criterion. In Fig. 6B, the FPZ size is approximately 0.45 mm.

As stated in literature (Kumar et al., 2011), the K-dominance zone r_k is defined as the distance from the crack tip where the singular stresses (eq. 3) represent 90-95 % of the normal stresses. Theoretically, if this condition is accomplished, then the stress state is governed by one parameter (SIF). In our unconfined tests, a conservative value is $r_k \approx 0.25 \text{ mm}$ obtained by FE stress analysis in Fig. 6B, about 2 times lower than the FPZ size defined by Schmidt criterion. It follows that fracture conditions for unconfined tests could be dominated by more than one parameter.

On the other hand, it seems possible that Schmidt's formula used to calculate the FPZ size under confined conditions might be invalid because of two reasons:

I- The method is valid if the SIF dominates the stress field. Previous studies have shown the significance of stress state description in the determination of FPZ. For example, Ayatollohi et al. (2014) show a method to calculate the FPZ size considering two parameters (K_I and the second non-singular stress term in William's equation). Furthermore, Schmidt's criterion neglects all stress components, except the normal stress in the plane of the notch. In a recent research, Nejati et al. (2020) proposed an energy-based redefinition of K-dominance to consider all components of stress-strain field. As previously stated, the compressive stresses in our confined tests prevent the FPZ development, decreasing the tensile stressed zone. Thus, a multiparametric fracture mechanics approach may be more appropriate to describe the FPZ behavior against confinement.

II- The method used the unconfined TS as a strength parameter, yet, it has been shown that this parameter is dependent upon the loading path and triaxial state (confined extension) (Patel and Martin, 2018). Liu et al. (2021) tested granite rock with cylindrical samples under triaxial conditions ($\sigma_1 = \sigma_2$ in compression, σ_3 in tension) and reported an increase of 20 % in TS from 0 MPa to 6 MPa confining stress, and an increase of 30 % in TS from 6 MPa to 12 MPa confining stress. Lan et al. (2019) carried out tests in shale rocks by using dog-bone samples and they found that from 0 MPa to 25 MPa confinement the tensile strength increases more than 2 times. In contrast, Z. Liu et al. (2019) reported results for quartz sandstone in cylindrical samples ($\sigma_1 = \sigma_2$ in compression, σ_3 in tension) and observed a decrease of 50 % in TS from unconfined to 12 MPa confinement. Some authors also reported experimental evidence of increasing strain bearing capacity under confined conditions (Liu et al., 2019; Patel and Martin, 2018; Zeng et al., 2019).

Then, the FPZ size calculated for the UC condition could be dependent on the triaxial state in near the crack-tip field stress, and the tensile strength sensitivity against the stress state. It may be argued that one of the reasons for increasing fracture toughness is the enhancement of both tensile strength and strain bearing capacity as confinement increases.

Input parameter	High confinement (HC)	Middle confinement (MC)	Unconfined (UC)
Differential break pressure (MPa)	11.8	9.3	7.9
Confining pressure (MPa)	70.5	20	0
Experimental K_{IC} (MPa.m ^{0.5})	1.15	0.8	0.75
Crack ratio a/D	0.1		
Young's Moduli (GPa)	45		
Poisson's Ratio	0.18		

Table 2: Input parameter to obtain stress distribution around the crack tip.

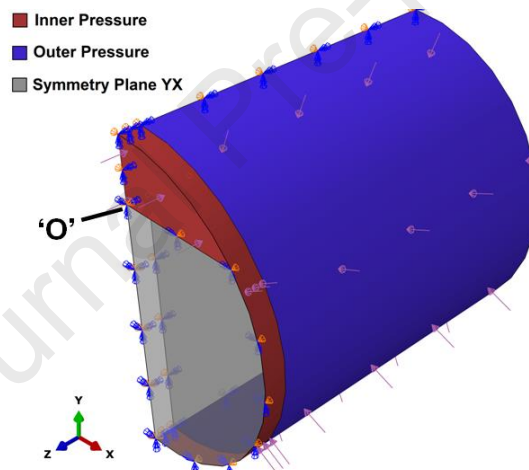


Figure 5: Loading condition used in SIF determination under confining pressure. The point 'O' is a reference for stress analysis near the crack tip (Antinao Fuentealba et al., 2022).

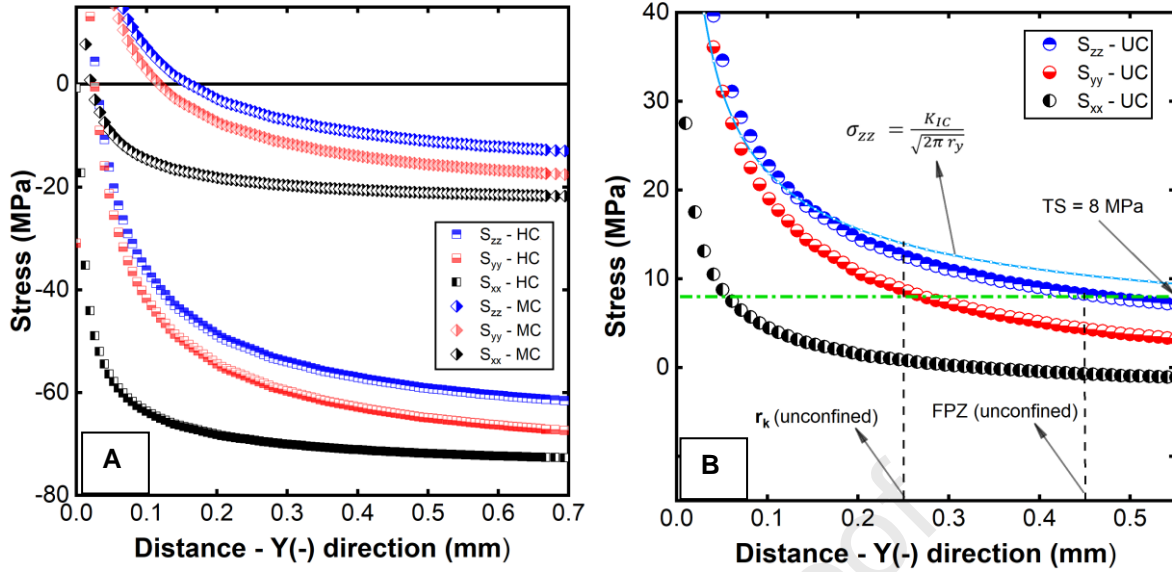


Figure 6: Principal stress distributions along Y(-) direction for: A) High Confinement (HC) and middle confinement (MC) condition B) Unconfined (UC); r_k is the dominance zone of the SIF for this condition. Positive stresses correspond to tension states.

Regarding the crack-tip stresses under HC and MC conditions, it was not possible to define an accurate FPZ size due to the lack of accurate stress values in that zone. Considering Schmidt's criterion, we do know it is smaller than $r_y \lesssim 0.025$ mm for HC tests, and $r_y \lesssim 0.1$ mm for the MC condition (Antinao Fuentealba et al. (Antinao Fuentealba et al., 2022), mesh elements near the crack tip have a 0.01 mm resolution. Fig. 6 is an enlarged image of Fig. 5A, where the FPZ size estimations for both cases can be seen. The red zone represents the crack tip front along the y-direction, with a compression-tensile stress state.

Therefore, K-dominance cannot be ensured, and fracture toughness under confinement conditions would not be accurately assessed by the one-parameter approach. The effect of non-singular parameters, the full description of the stress field under confined conditions in RBSN fracture tests, and its relationship with FPZ size are issues for future research.

Conceptually, it has been interpreted that the FPZ size decreases with confinement (P_c). For instance, considering Schmidt's criterion and Mode I crack tip stresses ($\theta = 0$), if confinement is imposed, then the FPZ tends to decrease with confinement (H. P. Rossmannith, 1983; Ko and Kemeny, 2007). Models based on the cohesive zone (CZ) have been used to analyze the effect of confinement on rock toughness. Hashida (1993), Fialko and Rubin (1997) used this approach to analyze the effect of compressive stresses in hydraulic fracture. They showed that increasing confinement reduces the size of CZ as well as increasing toughness. Following this work, Yue et al. (2020) extended the analysis to take fluid lag into account. They concluded that this phenomenon, along with confining pressure, were the reasons for increased down-well rock toughness but did not investigate the mechanisms.

Our analysis revealed that the compressive stresses near the crack tip under HC and MC conditions (Fig. 6A - 7) dominate along y-directions, suggesting that as P_c increases, the tensile stressed zone is reduced. Notably, the triaxially stressed tension-compression zone is one order larger for the MC condition than for the HC condition. These results are consistent with previous studies, although the inverse trend between FPZ size and P_c could not be fully established under linear elastic fracture mechanics (LEFM) conditions.

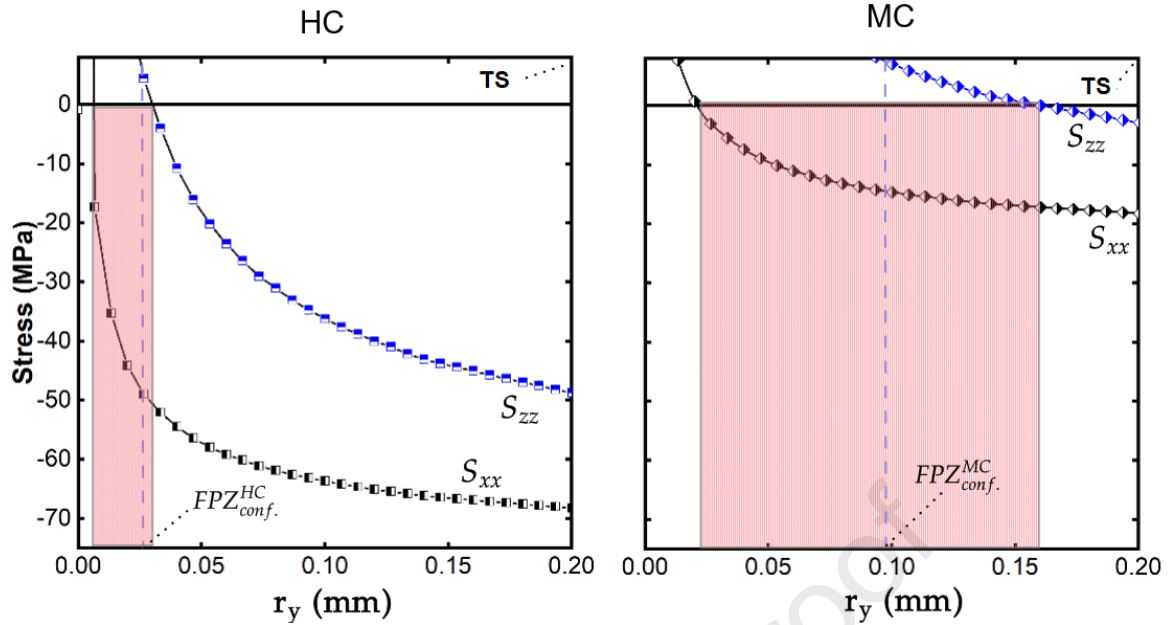


Figure 7. Principal stress distributions along Y (-) direction for High Confinement (HC) and middle confinement (MC) conditions. Tensile strength (TS) is the limit of stress axis. FPZ sizes are estimated from Schmidt's criterion.

3.2.1. Rock toughening mechanisms under confinement

The compressive stress field around the crack tip may modify the rock microcracking process. This is due to the phenomena of crack closure and initiation, which have been widely demonstrated in uniaxial and triaxial tests (Iferobia and Ahmad, 2020). They can be described according to different ratios of crack stress threshold with respect to the axial peak stress reached in triaxial tests.

During fracture tests, whereas the loading progresses, the material is feasibly to be populated with microcracks driven by deviatoric stresses outside of tension stressed zone (Fig. 7). According to the principles of toughening in rocks, microcracks are a source of toughness enhancement. Thus, they could act as a mechanism for increasing toughness, particularly if cohesionless microcracking is observed in confined tests. Beside, cohesionless and closed microcracks could trigger frictional forces between rock grains, restraining their movement. This mechanism was proposed by Liu et al. (2021) to explain the dependence of tensile strength on confinement.

Under deviatoric stress fields, microcrack toughening can synergistically occur alongside mechanisms such as ligamentary bridging and frictional interlocking, which are known as a toughening mechanism (Hashida et al., 1993; Swanson, 1987). Supporting this concept, in another study, Lou et al. (2017) conducted laboratory-scale HF experiments in outcrop sandstone cubes under different confinement conditions. They measured acoustic events mostly related with shear microcracking before the fracture initiation.

Our FE model results clearly show that the region near the crack tip predominantly experiences tensile stress, while compressive stresses are more prevalent outside this region. Figure 7 demonstrates that the position ' r_y ', where compression dominates, is influenced by the confining pressure. Although the definition of the fracture process zone (FPZ) under confinement is not yet clear, these findings align with previous studies and suggest that the fracture behavior observed in our confined fracture tests is governed by a hybrid mechanism. This mechanism involves microcracking toughening within the fracture process zone (FPZ) and a frictional mechanism associated with the closure of microcracks outside the FPZ.

Nevertheless, it is important to note that the occurrence of hybrid failure is strongly influenced by factors such as the magnitude of confinement, the nucleation and propagation of non-cohesive microcracks, and the attainment of the crack stress threshold.

Future research endeavors are aimed at testing and contrasting this hypothesis through acoustic event measurements in an experimental level. Our hypothesis is that analyzing acoustic emissions from microcracking during loading and fracture events can provide valuable insights into potential tensile or shear mechanisms occurring at the crack tip. Furthermore, we will align fracture mechanics models with failure envelopes derived from triaxial tests influenced by another research paper (Leith et al., 2014). By conducting these investigations, we aim to gain further understanding of the underlying mechanisms governing confined fracture behavior.

3.3. Reduction in fracture toughness due to water weakening

It has been shown that water-weakening mechanisms can be quantified as a function of fluid content (Zhou et al., 2018). In order to minimize the effect of water-weakening mechanisms (Antinao Fuentealba et al., 2020a; Chen et al., 2019), the samples were coated with water-proof paint, as shown in Section 2. This allows minimizing the contact area between the fracture fluid and the sample. The fluid could penetrate during the loading time, which may induce water-weakening and stress corrosion mechanisms. According to some studies, an empirical relationship between fluid content and fracture toughness should be a function of the type of fluid, time of rock-fluid contact, mineralogy, and petrophysical properties like permeability (Zhou et al., 2018). In this scenario, the consensus is that water-based fluids induce a decrease in mechanical rock properties (Wong et al., 2016). In particular, the more water content in the rock matrix, the more reduction in fracture toughness.

In Antinao Fuentealba et al. (2020a), uncoated samples were soaked for 24 hours in deionized water, gaining about 2.5-3 % of water content before atmospheric fracture tests. K_{IC} decreased 70 %. Linearizing this behavior, the toughness rate reduction due to water-weakening was about 0.02 MPa.m^{1/2}/h. In the present study, samples were loaded until break while water was in contact with the crack tip, during 10-20 min (Fig. 5B in Antinao Fuentealba et al. (Antinao Fuentealba et al., 2022)). Considering the aforementioned toughness reduction rate, the reduction of toughness due to water-weakening is smaller than 0.1 % for samples under high confinement conditions. In other words, the water content gained during loading times in our tests has a negligible effect on toughness. To check this, water content gained at different times was measured.

Unnotched samples were tested under 0 MPa and 50 MPa confinement, with the size of contact area between fluid and rock equivalent to that in samples used in fracture tests ($a/D=0.1$). This was done by eliminating the coating paint with diamond wire, using the method shown in Section 2, avoiding the creation of a notch (Fig. 8A). Differential pressures between chambers were similar to the rupture differential pressures in experimental tests, applied for short (15-20 min) and long (1-72 h) loading times (Antinao Fuentealba et al., 2022). Fully coated samples without notches were also tested in similar conditions. Samples were weighed before and after each test (accuracy 0.0001 g) to measure water gained. Fig. 9 shows results. It is noted that:

- Without confinement, saturation (0.3 % of water content) was reached after 30 h.
- Full-coated samples under confinement gained 0.1 % in 4hs. This means that coating allows some fluid penetration.
- Under confined conditions for longer periods, samples gained 0.15-0.4 % water in 1-4 h, and 1.2 % after 50 h.
- For shorter periods (15-20 min), representative of fracture tests, both confined and unconfined samples gained 0.005 %-0.05 % water.

These results show that coating minimizes the interaction of the rock with the fracture fluid, but may not be efficient for longer periods. Microscopic inspection of coating in samples confirmed that air micropores due to coat application might allow fluids to reach the rock surface. In any case, results show that during the time scales of our fracture tests, gained water has a negligible effect on toughness.

The influence of stress corrosion on rock toughness in subcritical conditions is mostly unknown. According to previous studies, it is mainly controlled by time, type of fracture fluid, chemical conditions (pH, salinity, temperature) and rock mineralogy (Chen et al., 2020). Once again, because of the low content of fluid gained in our short fracture test times, toughness reduction by stress corrosion can be neglected. The methodology used in the present study is consistent with that presented in the literature. For instance, Chen et al. (2019) used coated double-torsion samples to investigate K_I - propagation velocity curves in carbonate-rich shale rocks, by using deionized water. In their research, neither fracture toughness nor stress corrosion index for coated and uncoated samples were sensitive to water content gained during loading times (about 7 min in fracture tests, 50 min in stress corrosion tests).

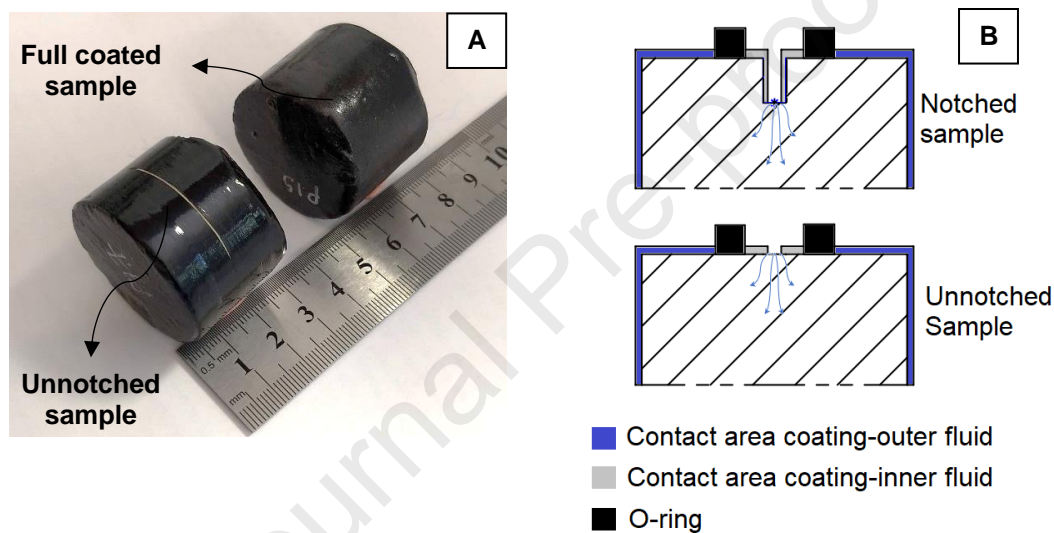


Figure 8: A) Sample used to evaluate rock-fluid interaction. B) Schematic of interaction between water and notched-unnotched samples.

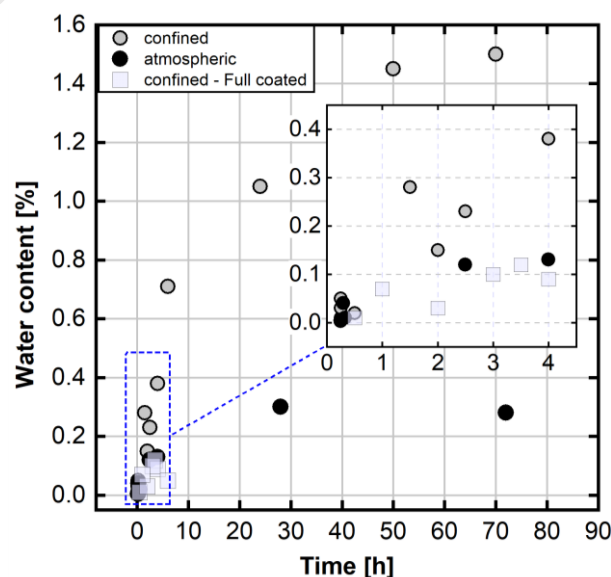


Figure 9: Water content gained in rock samples in different conditions.

3.4. Study limitations and future research

As previously discussed in Antinao Fuentealba et al. (2020a), we revisit the sources of scatter in the experimental data, emphasizing the need for further research in these areas.

- A) Rock homogeneity in physical properties: In Section 2, it was mentioned that specimens were extracted from block outcrops and subsequently machined using a drill bit. As these blocks were sampled from various locations within the outcrops, they may exhibit variations in the amount and types of defects (porosity, fluid content, chemical/mineralogical composition, presence of defects, grain size, etc.). It was argued that these defects were the main source of scatter in toughness results. Consequently, the measured toughness of the samples is influenced by these factors, potentially resulting in variations of their physical properties.
- B) Crack tip radius (Fig. 3C): the notch used in our experiments was about 0.4 mm in radius, and stress intensity factor was determined by using a zero-thickness approach in numerical models. The relative size of FPZ with respect to the notch tip radius could have an influence in our K_{IC} measurements (S. Zhang et al., 2020) and it could also modify the intensity of singularity near the crack tip (Saboori et al., 2016). Additional research is needed to evaluate the effect of notch radius on SIF.
- C) The potential density of microcracks induced during the tests could be influenced by the presence of preexisting microcracks in the samples. Ensuring identical microstructural properties for all specimens is challenging. Consequently, variations in the density of preexisting microcracks may contribute to scattering in fracture toughness measurements. Since the mechanisms discussed are strongly influenced by these inherent defects, it is crucial for future methods to strive for consistent preexisting defects prior to conducting any tests.
- D) Geometry dependency: In Section 3.2, it has been proposed that a multiparametric fracture mechanics approach could be more appropriate for describing the fracture tests. While extensive research has been conducted under atmospheric conditions, there is a noticeable gap in research regarding confined conditions. To address this gap, future studies will employ a well-known method called the over-deterministic method to determine the non-singular parameters (Ayatollahi and Nejati, 2011). By utilizing this method, a more comprehensive understanding of the geometry-dependent behavior under confined conditions can be achieved.
- E) Effect of anisotropy: All our rock samples contain bedding planes. However, the constitutive material model used in this article is isotropic and homogenous. The influence of the variation of Poisson's and Young's moduli on SIF has been neglected. The stress component S_{yy} in the ligament shown in Fig. 6 is independent of anisotropy, while S_{xx} and S_{zz} depend on anisotropy ratios, bedding angle orientation, and loading configuration (Nejati et al., 2019). Future FE models could include anisotropy to better understand fracture behavior of these rocks.

4. CONCLUSIONS

Fracture toughness of calcareous rock samples from Vaca Muerta formation was determined under confined conditions by using RBSN samples. The experimental set up was composed of two chambers (an inner chamber and an outer one), both isolated by elastomer O-rings (NBR). The inner chamber allowed placing the sample and inducing the hydraulic driving force in the notch, and the external chamber allowed inducing the confining pressure.

A major effect of confinement pressure is observed: tests carried out at well-bottom pressures lead to apparent rock toughness doubling those for tests carried out at atmospheric pressure. It is concluded that increasing triaxial pressure confinement allows to accurately model the conditions of the rock in reservoir conditions.

The stress analysis near the crack tip showed that, in the unconfined tests, the FPZ size was about 0.45 mm, but the K-dominance was reached at distances in the order of 0.25 mm. These suggest that fracture behavior in atmospheric tests was governed by more than one fracture parameter. The stresses in the highly confined tests were compressive as soon as the distance from the crack tip was larger than 1×10^{-2} mm. This implies that rock fracture was dominated by compressive stresses, presumably leading to a decrease in the FPZ size as confinement increases. The magnitude of deviatoric stresses near the crack tip could activate the crack closure and multiple microcracking mechanisms, which synergistically, both might act as toughening mechanisms during rock fracture.

Future studies will address microcrack-toughening mechanisms induced by deviatoric stresses through acoustic emission measurements. Additionally, stress fields will be described using a multiparametric fracture mechanics approach under confined conditions.

ACKNOWLEDGEMENTS

This research was partly funded by CONICET (Consejo Nacional de Investigaciones Científicas y Técnicas, Argentina), and Agencia Nacional de Promoción Científica y Tecnológica, Argentina, PICT-2017-2489 and PICT-Startup 2020-00011. Authors thank Ricardo Ramos from SOLAER S.A. for motivation and funding for this research, and Ariel Sánchez Camus from TECTIONS S.A. for helpful discussions and encouragement.

REFERENCES

- Abou-Sayed, A.S., Brechtel, C.E., Clifton, R.J., 1978. In situ stress determination by hydrofracturing: A fracture mechanics approach. *J. Geophys. Res.* 83, 2851. <https://doi.org/10.1029/jb083ib06p02851>
- Al-Shayea, N.A., Khan, K., Abduljauwad, S.N., 2000. Effects of confining pressure and temperature on mixed-mode (I-II) fracture toughness of a limestone rock. *Int. J. Rock Mech. Min. Sci.* 37, 629–643. [https://doi.org/https://doi.org/10.1016/S1365-1609\(00\)00003-4](https://doi.org/https://doi.org/10.1016/S1365-1609(00)00003-4)
- Aliha, M.R.M., Mahdavi, E., Ayatollahi, M.R., 2016. The Influence of Specimen Type on Tensile Fracture Toughness of Rock Materials. *Pure Appl. Geophys.* 174, 1237–1253. <https://doi.org/10.1007/s00024-016-1458-x>
- Amadei, B., Stephansson, O., 1997. *Rock Stress and Its Measurement*.
- Antinao Fuentealba, F.J., Bianchi, L.N., Otegui, J.L., Bianchi, G.L., 2022. Accurate experimental determination of rock fracture toughness under simulated reservoir confining. *Theor. Appl. Fract. Mech.* 120. <https://doi.org/10.1016/j.tafmec.2022.103425>
- Antinao Fuentealba, F.J., Otegui, J.L., Bianchi, G.L., 2020a. Improved technique for toughness testing of shale rocks. *Eng. Fract. Mech.* 235, 13. <https://doi.org/10.1016/j.engfracmech.2020.107182>
- Antinao Fuentealba, F.J., Romero, J.J., Otegui, J.L., Bianchi, G.L., 2020b. Device for rock fracture toughness testing under hydrocarbon reservoir conditions. *Theor. Appl. Fract. Mech.* 109, 102718. <https://doi.org/10.1016/j.tafmec.2020.102718>
- Ayatollahi, M.R., Akbardoost, J., 2014. Size and geometry effects on rock fracture toughness: Mode I fracture. *Rock Mech. Rock Eng.* 47, 677–687. <https://doi.org/10.1007/s00603-013-0430-7>
- Ayatollahi, M.R., Nejati, M., 2011. An over-deterministic method for calculation of coefficients of crack tip asymptotic field from finite element analysis. *Fatigue Fract. Eng. Mater. Struct.* 34, 159–176. <https://doi.org/10.1111/j.1460-2695.2010.01504.x>
- Balme, M.R., Rocchi, V., Jones, C., Sammonds, P.R., Meredith, P.G., Boon, S., 2004. Fracture toughness measurements on igneous rocks using a high-pressure, high-temperature rock fracture mechanics cell 132, 159–172. [https://doi.org/https://doi.org/10.1016/S0377-0273\(03\)00343-3](https://doi.org/https://doi.org/10.1016/S0377-0273(03)00343-3)
- Chen, M., Guo, T., Qu, Z., Sheng, M., Mu, L., 2022. Numerical investigation into hydraulic fracture initiation and breakdown pressures considering wellbore compliance based on the boundary element method. *J. Pet. Sci. Eng.* 211, 110162. <https://doi.org/10.1016/j.petrol.2022.110162>
- Chen, X., Eichhubl, P., Olson, J.E., Dewers, T.A., 2020. Salinity, pH, and temperature controls on

- fracture mechanical properties of three shales and their implications for fracture growth in chemically reactive fluid environments. *Geomech. Energy Environ.* 21, 100140. <https://doi.org/10.1016/j.gete.2019.100140>
- Chen, X., Eichhubl, P., Olson, J.E., Dewers, T.A., 2019. Effect of Water on Fracture Mechanical Properties of Shales. *J. Geophys. Res. Solid Earth* 125, 2428–2444. <https://doi.org/10.1029/2018JB016479>
- Dai, F., Wei, M.D., Xu, N.W., Zhao, T., Xu, Y., 2015. Numerical investigation of the progressive fracture mechanisms of four ISRM-suggested specimens for determining the mode I fracture toughness of rocks. *Comput. Geotech.* 69, 424–441. <https://doi.org/10.1016/j.compgeo.2015.06.011>
- Dassault Systèmes, 2014. Abaqus documentation V6.14. Dassault Systèmes Simulia Corp.
- Dresen, G., Stanchits, S., Rybacki, E., 2010. Borehole breakout evolution through acoustic emission location analysis. *Int. J. Rock Mech. Min. Sci.* 47, 426–435. <https://doi.org/10.1016/j.ijrmms.2009.12.010>
- Dutler, N., Nejati, M., Valley, B., Amann, F., Molinari, G., 2018. On the link between fracture toughness, tensile strength, and fracture process zone in anisotropic rocks. *Eng. Fract. Mech.* 201, 56–79. <https://doi.org/10.1016/j.engfracmech.2018.08.017>
- Economides, M.J., Kenneth, G.N., 2000. *Reservoir Stimulation*, 3rd ed. Wiley.
- Fan, Y., Zhu, Z., Zhao, Y., Zhou, C., Zhang, X., 2019. The effects of some parameters on perforation tip initiation pressures in hydraulic fracturing. *J. Pet. Sci. Eng.* 176, 1053–1060. <https://doi.org/10.1016/j.petrol.2019.02.028>
- Fialko, Y.A., Rubin, A.M., 1997. Numerical simulation of high-pressure rock tensile fracture experiments: Evidence of an increase in fracture energy with pressure? *J. Geophys. Res. Solid Earth* 102, 5231–5242. <https://doi.org/10.1029/96jb03859>
- Frydman, M., Pacheco, F., Pastor, J., Canesin, F.C., Caniggia, J., Davey, H., 2016. Comprehensive determination of the far-field earth stresses for rocks with anisotropy in tectonic environment. *Soc. Pet. Eng. - SPE Argentina Explor. Prod. Unconv. Resour. Symp.* 1–14. <https://doi.org/10.2118/180965-ms>
- Funatsu, T., Seto, M., Shimada, H., Matsui, K., Kuruppu, M., 2004. Combined effects of increasing temperature and confining pressure on the fracture toughness of clay bearing rocks. *Int. J. Rock Mech. Min. Sci.* 41, 927–938. <https://doi.org/10.1016/j.ijrmms.2004.02.008>
- Gao, G., Wang, C., Zhou, H., Wang, P., 2020. Modified fracture mechanics approach for hydraulic fracturing stress measurements. *Geofluids* 2020. <https://doi.org/10.1155/2020/8860163>
- Garg, P., Zafar, S., Hedayat, A., Moradian, O.Z., Griffiths, D. V., 2023. A novel methodology for characterizing fracture process zone evolution in Barre granite specimens under mode I loading. *Theor. Appl. Fract. Mech.* 123, 103727. <https://doi.org/10.1016/j.tafmec.2022.103727>
- Gehne, S., Forbes Inskip, N.D., Benson, P.M., Meredith, P.G., Koor, N., 2020. Fluid-Driven Tensile Fracture and Fracture Toughness in Nash Point Shale at Elevated Pressure. *J. Geophys. Res. Solid Earth* 125, 1–11. <https://doi.org/10.1029/2019JB018971>
- Ghanbari, N., Hosseini, M., Saghafiyazdi, M., 2019. Effects of temperature and confining pressure on the mode I and mode II fracture toughness of cement mortar. *Theor. Appl. Fract. Mech.* 104. <https://doi.org/10.1016/j.tafmec.2019.102361>
- Green, D.J., 2018. *Transformation Toughening Of Ceramics*, 1st ed. CRC Press.
- Gudmundsson, A., 2011. *Rock Fractures in Geological Processes*, Rock Fractures in Geological Processes. Cambridge University Press. <https://doi.org/10.1017/cbo9780511975684>
- H. P. Rossmanith, 1983. *Rock Fracture Mechanics*. Springer Vienna. <https://doi.org/10.1007/978-3-7091-2750-6>
- Hammouda, M.M.I., 2022. Mixed-mode I/II stress intensity factors for frictional centrally cracked Brazilian disk with confining pressure. *Fatigue Fract. Eng. Mater. Struct.* 45, 1830–1841. <https://doi.org/10.1111/ffe.13703>
- Hashida, T., Oghikubo, H., Takahashi, H., Shoji, T., 1993. Numerical simulation with experimental verification of the fracture behavior in granite under confining pressures based on the tension-softening model. *Int. J. Fract.* 59, 227–244.
- Heng, S., Li, X., Zhang, X., Li, Z., 2021. Mechanisms for the control of the complex propagation behaviour of hydraulic fractures in shale. *J. Pet. Sci. Eng.* 200. <https://doi.org/10.1016/j.petrol.2021.108417>
- Hertzberg, R., Vinci, R.P., Hertzberg, J.L., 2012. *Deformation and Fracture Mechanics of Engineering Materials*, 5th ed. John Wiley & Sons.
- Hoek, E., Martin, C.D., 2014. Fracture initiation and propagation in intact rock - A review. *J. Rock Mech. Geotech. Eng.* 6, 287–300. <https://doi.org/10.1016/j.jrmge.2014.06.001>
- Hou, C., Wang, Zhiyong, Liang, W., Yu, H., Wang, Zhihua, 2017. Investigation of the effects of confining

- pressure on SIFs and T-stress for CCBD specimens using the XFEM and the interaction integral method. *Eng. Fract. Mech.* 178, 279–300. <https://doi.org/10.1016/j.engfracmech.2017.03.049>
- Iferobia, C.C., Ahmad, M., 2020. A review on the experimental techniques and applications in the geomechanical evaluation of shale gas reservoirs. *J. Nat. Gas Sci. Eng.* 74, 103090. <https://doi.org/10.1016/j.jngse.2019.103090>
- Jaeger, C., 2007. *Fundamentals of rock mechanics*. Methuen, London.
- Jeffrey, R.G., 2007. The Combined Effect of Fluid Lag and Fracture Toughness on Hydraulic Fracture Propagation 269–276. <https://doi.org/10.2118/18957-ms>
- Jin, X., Shah, S.N., Roegiers, J.-C., Zhang, B., 2014. Fracability Evaluation in Shale Reservoirs - An Integrated Petrophysics and Geomechanics Approach. *SPE Hydraul. Fract. Technol. Conf.* <https://doi.org/10.2118/168589-MS>
- K. Broberg, 1999. *Cracks and Fracture*. Academic Press.
- Kataoka, M., Mahdavi, E., Funatsu, T., Takehara, T., Obara, Y., Fukui, K., Hashiba, K., 2017. Estimation of Mode I Fracture Toughness of Rock by Semi-Circular Bend Test under Confining Pressure Condition. *Procedia Eng.* 191, 886–893. <https://doi.org/10.1016/j.proeng.2017.05.258>
- Ko, T.Y., Kemeny, J., 2007. Effect of Confining Stress And Loading Rate On Fracture Toughness of Rocks. 1st Canada - U.S. Rock Mech. Symp.
- Kumar, B., Chitsiriphanit, S., Sun, C.T., 2011. Significance of K-dominance zone size and nonsingular stress field in brittle fracture. *Eng. Fract. Mech.* 78, 2042–2051. <https://doi.org/10.1016/j.engfracmech.2011.03.015>
- Lan, H., Chen, J., Macciotta, R., 2019. Universal confined tensile strength of intact rock. *Sci. Rep.* 9, 1–9. <https://doi.org/10.1038/s41598-019-42698-6>
- Lecampion, B., Bungler, A., Zhang, X., 2018. Numerical methods for hydraulic fracture propagation: A review of recent trends. *J. Nat. Gas Sci. Eng.* 49, 66–83. <https://doi.org/10.1016/j.jngse.2017.10.012>
- Li, C., Xie, H., Wang, J., 2020. Anisotropic characteristics of crack initiation and crack damage thresholds for shale. *Int. J. Rock Mech. Min. Sci.* 126, 104178. <https://doi.org/10.1016/j.ijrmms.2019.104178>
- Lin, H., Oh, J., Canbulat, I., Stacey, T.R., 2020. Experimental and Analytical Investigations of the Effect of Hole Size on Borehole Breakout Geometries for Estimation of In Situ Stresses. *Rock Mech. Rock Eng.* 53, 781–798. <https://doi.org/10.1007/s00603-019-01944-z>
- Liu, J., Li, Y., Qiao, L., 2022. Analytical Solutions of Stress Intensity Factors for a Centrally Cracked Brazilian Disc Considering Tangential Friction Effects. *Rock Mech. Rock Eng.* 55, 2459–2470. <https://doi.org/10.1007/s00603-021-02746-y>
- Liu, Y., Da Huang, ., Cen, D., Zhong, Z., Fengqiang Gong, ., Wu, Z., Yang, Y., 2021. Tensile Strength and Fracture Surface Morphology of Granite Under Confined Direct Tension Test. *Rock Mech. Rock Eng.* 1, 3. <https://doi.org/10.1007/s00603-021-02543-7>
- Liu, Z., Zhou, H., Zhang, W., Xie, S., Shao, J., 2019. A new experimental method for tensile property study of quartz sandstone under confining pressure. *Int. J. Rock Mech. Min. Sci.* 123, 104091. <https://doi.org/10.1016/j.ijrmms.2019.104091>
- Lou, Y., Zhang, G., Wang, X., 2017. Study on Fracture Mechanism of Hydraulic Fracturing in Sandstone by Acoustic Emission Parameters. *Procedia Eng.* 191, 291–298. <https://doi.org/10.1016/j.proeng.2017.05.184>
- Lu, Z., Lai, H., Zhou, L., Shen, Z., Ren, X., Li, X., 2022. Prediction of hydraulic fracture initiation pressure in a borehole based on a neural network model considering plastic critical distance. *Eng. Fract. Mech.* 274, 108779. <https://doi.org/10.1016/j.engfracmech.2022.108779>
- Massaro Sosa, A., 2019. Estudio Geomecánico Regional de la Formación Vaca Muerta y su Aplicación a los Reservorios No Convencionales del tipo Shale oil/gas. Instituto Tecnológico de Buenos Aires.
- Mcclure, M., Picone, M., Fowler, G., Ratcliff, D., Kang, C., Medam, S., Frantz, J., 2020. Nuances and Frequently Asked Questions in Field-Scale Hydraulic Fracture Modeling Data-driven and physics-based models. *SPE-199726-MS* 1–19.
- Meng, T., Zhang, D.H., Hu, Y., Jianlin, X., Sufang, S., Xiaoming, L., 2018. Study of the deformation characteristics and fracture criterion of the mixed mode fracture toughness of gypsum interlayers from Yunying salt cavern under a confining pressure. *J. Nat. Gas Sci. Eng.* 58, 1–14. <https://doi.org/10.1016/j.jngse.2018.07.020>
- Michael, A., Gupta, I., 2020. Analytical orientation criteria for drilling and completion-induced fracture initiation considering fluid infiltration from the wellbore. *J. Pet. Sci. Eng.* 190. <https://doi.org/10.1016/j.petrol.2020.107033>
- Mirabbasi, S.M., Ameri, M.J., Biglari, F.R., Shirzadi, A., 2020. Thermo-poroelastic wellbore strengthening modeling: An analytical approach based on fracture mechanics. *J. Pet. Sci. Eng.*

- 195, 107492. <https://doi.org/10.1016/j.petrol.2020.107492>
- Mohamadi, A., Behnia, M., Alneasan, M., 2021. Comparison of the classical and fracture mechanics approaches to determine in situ stress/hydrofracturing method. *Bull. Eng. Geol. Environ.* 80, 3833–3851. <https://doi.org/10.1007/s10064-021-02184-8>
- Müller, W., 1986. Brittle crack growth in rocks. *Pure Appl. Geophys.* 124, 693–709. <https://doi.org/10.1007/BF00879605>
- Nejati, M., Aminzadeh, A., Saar, M.O., Driesner, T., 2019. Modified semi-circular bend test to determine the fracture toughness of anisotropic rocks. *Eng. Fract. Mech.* 213, 153–171. <https://doi.org/10.1016/j.engfracmech.2019.03.008>
- Nejati, M., Ghouli, S., Ayatollahi, M.R., 2020. Crack tip asymptotic field and K-dominant region for anisotropic semi-circular bend specimen. *Theor. Appl. Fract. Mech.* 109, 102640. <https://doi.org/10.1016/j.tafmec.2020.102640>
- Pakdaman, A.M., Moosavi, M., Mohammadi, S., 2019. Experimental and numerical investigation into the methods of determination of mode I static fracture toughness of rocks. *Theor. Appl. Fract. Mech.* 100, 154–170. <https://doi.org/10.1016/j.tafmec.2019.01.001>
- Pan, R., Zhang, G., Li, S., Zheng, X., Xu, C., Fan, Z., 2021. Influence of the fracture process zone on fracture propagation mode in layered rocks. *J. Pet. Sci. Eng.* 202, 108524. <https://doi.org/10.1016/j.petrol.2021.108524>
- Patel, S., Martin, C.D., 2018. Application of Flattened Brazilian Test to Investigate Rocks Under Confined Extension. *Rock Mech. Rock Eng.* 51, 3719–3736. <https://doi.org/10.1007/s00603-018-1559-1>
- Paterson, M.S., Wong, T., 2005. *Experimental Rock Deformation: the Brittle Field*. Springer.
- Perras, M.A., Diederichs, M.S., 2014. A Review of the Tensile Strength of Rock: Concepts and Testing. *Geotech. Geol. Eng.* 32, 525–546. <https://doi.org/10.1007/s10706-014-9732-0>
- Rahimzadeh Kivi, I., Ameri, M., Molladavoodi, H., 2018. Shale brittleness evaluation based on energy balance analysis of stress-strain curves. *J. Pet. Sci. Eng.* 167, 1–19. <https://doi.org/10.1016/j.petrol.2018.03.061>
- Razavi, O., Vajargah, A.K., van Oort, E., Aldin, M., 2017. Comprehensive analysis of initiation and propagation pressures in drilling induced fractures. *J. Pet. Sci. Eng.* 149, 228–243. <https://doi.org/10.1016/j.petrol.2016.10.039>
- Roegiers, J.C., Zhao, X.L., 1991. Rock fracture tests in simulated downhole conditions. 32nd U.S. Symp. Rock Mech. *USRMS 1991 ARMA-91-22*, 221–230.
- Saboori, B., Ayatollahi, M.R., Torabi, A.R., Berto, F., 2016. Mixed mode I/III brittle fracture in round-tip V-notches. *Theor. Appl. Fract. Mech.* 83, 135–151. <https://doi.org/10.1016/j.tafmec.2015.12.002>
- Sapora, A., Spagnoli, A., Susmel, L., Cornetti, P., 2023. A simplified approach to hydraulic fracturing of rocks based on Finite Fracture Mechanics. *Fatigue Fract. Eng. Mater. Struct.* <https://doi.org/10.1111/ffe.14069>
- Schmidt, R.A., 1980. A Microcrack Model And Its Significance to Hydraulic Fracturing And Fracture Toughness Testing. 21st U.S. Symp. Rock Mech.
- Sharifigaliuk, H., Mahmood, S.M., Ahmad, M., Rezaee, R., 2021. Use of Outcrop as Substitute for Subsurface Shale: Current Understanding of Similarities, Discrepancies, and Associated Challenges. *Energy and Fuels* 35, 9151–9164. <https://doi.org/10.1021/acs.energyfuels.1c00598>
- Shlyapobersky, J., 1985. Energy analysis of hydraulic fracturing. 26th US Symp. Rock Mech. 539–546.
- Shlyapobersky, J., Chudnovsky, A., 1994. Review of recent developments in fracture mechanics with petroleum engineering applications, in: Paper SPE 28074 Presented at the Eurock SPE/ISRM Rock Mechanics in Petroleum Engineering Conference. pp. 381–389.
- Shlyapobersky, J., Walhaug, W.W., Sheffield, R.E., Huckabee, P.T., 1988. Field determination of fracturing parameters for overpressure calibrated design of hydraulic fracturing. *Soc. Pet. Eng. AIME, SPE PI.* <https://doi.org/10.2118/18195-ms>
- Smith, M.B., Montgomery, C.T., 2015. *Hydraulic fracturing*, 1st ed. CRC Press.
- Swanson, P.L., 1987. TENSILE FRACTURE RESISTANCE MECHANISMS IN BRITTLE POLYCRYSTALS: AN ULTRASONICS AND IN SITU MICROSCOPY INVESTIGATION. *J. Geophys. Res. Solid Earth* 92, 8015–8036. <https://doi.org/https://doi.org/10.1029/JB092iB08p08015>
- Taheri, A., Zhang, Y., Munoz, H., 2020. Performance of rock crack stress thresholds determination criteria and investigating strength and confining pressure effects. *Constr. Build. Mater.* 243, 118263. <https://doi.org/10.1016/j.conbuildmat.2020.118263>
- Thiercelin, M., 1989. Fracture toughness and hydraulic fracturing. *Int. J. Rock Mech. Min. Sci.* 26, 177–183. [https://doi.org/10.1016/0148-9062\(89\)91967-0](https://doi.org/10.1016/0148-9062(89)91967-0)
- Van Dam, D.B., De Pater, C.J., 2001. Roughness of hydraulic fractures: Importance of in-situ stress and

- tip processes. *SPE J.* 6, 4–13. <https://doi.org/10.2118/68775-PA>
- Vásárhelyi, B., 1997. Influence of pressure on the crack propagation under mode I loading in anisotropic gneiss. *Rock Mech. Rock Eng.* 30, 59–64. <https://doi.org/10.1007/bf01020113>
- Wang, H.Y., 2015. Numerical modeling of non-planar hydraulic fracture propagation in brittle and ductile rocks using XFEM with cohesive zone method. *J. Pet. Sci. Eng.* 135, 127–140. <https://doi.org/10.1016/j.petrol.2015.08.010>
- Wang, W., Olson, J.E., Prodanović, M., Schultz, R.A., 2018. Interaction between cemented natural fractures and hydraulic fractures assessed by experiments and numerical simulations. *J. Pet. Sci. Eng.* 167, 506–516. <https://doi.org/10.1016/j.petrol.2018.03.095>
- Wei, M.D., Dai, F., Liu, Y., Li, A., Yan, Z., 2021. Influences of Loading Method and Notch Type on Rock Fracture Toughness Measurements: From the Perspectives of T-Stress and Fracture Process Zone. *Rock Mech. Rock Eng.* <https://doi.org/10.1007/s00603-021-02541-9>
- Winter, R.B., 1983. Bruchmechanische Gesteinsuntersuchungen mit dem Bezug zu hydraulischen Frac-Versuchen in Tiefbohrungen, Berichte des Instituts für Geophysik der Ruhr-Universität Bochum / A. Inst. für Geophysik.
- Wong, L.N.Y., Maruvanchery, V., Liu, G., 2016. Water effects on rock strength and stiffness degradation. *Acta Geotech.* 11, 713–737. <https://doi.org/10.1007/s11440-015-0407-7>
- Xu, X., Wu, S., Jin, A., Gao, Y., 2018. Review of the Relationships between Crack Initiation Stress, Mode I Fracture Toughness and Tensile Strength of Geo-Materials. *Int. J. Geomech.* 18, 04018136. [https://doi.org/10.1061/\(asce\)gm.1943-5622.0001227](https://doi.org/10.1061/(asce)gm.1943-5622.0001227)
- Yang, H., Krause, M., Renner, J., 2021. Determination of Fracture Toughness of Mode I Fractures from Three - Point Bending Tests at Elevated Confining Pressures. *Rock Mech. Rock Eng.* <https://doi.org/10.1007/s00603-021-02432-z>
- Yang, J., Lian, H., Li, L., 2021. Investigating the effect of confining pressure on fracture toughness of CO₂-saturated coals. *Eng. Fract. Mech.* 242. <https://doi.org/10.1016/j.engfracmech.2020.107496>
- Yew, C.H., Liu, G.H., 1993. The Fracture Tip and Critical Stress Intensity Factor of a Hydraulically Induced Fracture. *SPE Prod. Facil.* 8, 171–177. <https://doi.org/10.2118/22875-pa>
- Yoshioka, K., Zhang, Y., Lu, G., Bungler, A., Adachi, J., Bourdin, B., 2023. Improving the Accuracy of Fracture Toughness Measurement in Burst Experiments. *Rock Mech. Rock Eng.* 56, 427–436. <https://doi.org/10.1007/s00603-022-03097-y>
- Yue, K., Lee, H.P., Olson, J.E., Schultz, R.A., 2020. Apparent fracture toughness for LFM applications in hydraulic fracture modeling. *Eng. Fract. Mech.* 230, 106984. <https://doi.org/10.1016/j.engfracmech.2020.106984>
- Zeng, B., Huang, D., Ye, S., Chen, F., Zhu, T., Tu, Y., 2019. Triaxial extension tests on sandstone using a simple auxiliary apparatus. *Int. J. Rock Mech. Min. Sci.* 120, 29–40. <https://doi.org/10.1016/j.ijrmms.2019.06.006>
- Zhang, Q., Fan, X., Chen, P., Ma, T., Zeng, F., 2020. Geomechanical behaviors of shale after water absorption considering the combined effect of anisotropy and hydration. *Eng. Geol.* 269, 105547. <https://doi.org/10.1016/j.enggeo.2020.105547>
- Zhang, S., Wang, L., Gao, M., 2020. Experimental and Numerical Study of the Influence of Prefabricated Crack Width on the Fracture Toughness of NSCB Specimens. *Rock Mech. Rock Eng.* 53, 5133–5154. <https://doi.org/10.1007/s00603-020-02211-2>
- Zhong, R., Miska, S., Yu, M., Ozbayoglu, E., Takach, N., 2018. An integrated fluid flow and fracture mechanics model for wellbore strengthening. *J. Pet. Sci. Eng.* 167, 702–715. <https://doi.org/10.1016/j.petrol.2018.04.052>
- Zhou, Z., Cai, X., Ma, D., Cao, W., Chen, L., Zhou, J., 2018. Effects of water content on fracture and mechanical behavior of sandstone with a low clay mineral content. *Eng. Fract. Mech.* 193, 47–65. <https://doi.org/10.1016/j.engfracmech.2018.02.028>
- Zhu, D., Han, G., Zou, H., Cui, M., Liang, C., Yao, F., 2022. A Review of the Hydraulic Fracturing in Ductile Reservoirs: Theory, Simulation, and Experiment. Processes. <https://doi.org/10.3390/pr10102022>

Fracture toughness tests of shale outcrops: effects of confining pressure

Fabián J. Antinao Fuentealba^{*ad}, Gonzalo Blanco^{ab}, Leandro N. Bianchi^c, José L. Otegui^{ab},
Gustavo L. Bianchi^{ab}

^a Innovation for Energy and Environment, Malvinas Institute. Faculty of Engineering, National University of La Plata, Argentina.

^b National Scientific and Technical Research Council (CONICET), Argentina.

^c Solaer Ingeniería S.A, La Plata, Argentina.

Tections South S.A ^d

*corresponding author: fabian.antinao@ing.unlp.edu.ar

Highlights

- A Mode-I fluid-driven fracture toughness testing method has been developed.
- Confined K_{IC} was measured in Vaca Muerta carbonate-rich shale specimens.
- K_{IC} under confinement doubles unconfined fracture toughness laboratory results.
- Fracture process zone development was analyzed via finite-element crack tip stress analyses
- Microcracking induced by deviatoric stresses is a feasible mechanism for FPZ size and toughness variations

Fracture toughness tests of shale outcrops: effects of confining pressure

Fabián J. Antinao Fuentealba^{*ad}, Gonzalo Blanco^{ab}, Leandro N. Bianchi^c, José L. Otegui^{ab},
Gustavo L. Bianchi^{ab}

^a Innovation for Energy and Environment, Malvinas Institute. Faculty of Engineering, National University of La Plata, Argentina.

^b National Scientific and Technical Research Council (CONICET), Argentina.

^c Solaer Ingeniería S.A, La Plata, Argentina.

Tections South S.A ^d

*corresponding author: fabian.antinao@ing.unlp.edu.ar

Declaration of Competing Interest

The authors declare that they have no known competing financial interests or personal relationships that could have appeared to influence the work reported in this paper.